Carbohydrate Polymers 75 (2009) 712–718

Contents lists available at ScienceDirect

Carbohydrate Polymers

journal homepage: www.elsevier.com/locate/carbpol

Thermoplastic corn starch/clay hybrids: Effect of clay type and content on physical properties

N.F. Magalhães, C.T. Andrade *

Instituto de Macromoléculas Professora Eloisa Mano, Universidade Federal do Rio de Janeiro, Centro de Tecnologia, Bloco J, P.O. Box 68525, Rio de Janeiro, RJ 21945-970, Brazil

ARTICLE INFO

Article history:
Received 3 June 2008
Received in revised form 27 August 2008
Accepted 15 September 2008
Available online 25 September 2008

Keywords:
Thermoplastic starch
Clay
Hybrids
Crystallinity
Aging
Biodegradation

ABSTRACT

Thermoplastic corn starch (TPS) hybrids, plasticized with glycerol and reinforced with two types of clay (sodium montmorillonite and Cloisite® 30B), were prepared by melt-extrusion. Scanning electron microscopy was used to visualize extrudates morphology. The effects of clay content and of glycerol content on the physical properties of extrudates were evaluated. As determined by contact angle measurements and X-ray diffraction, the increase in glycerol content led to materials with higher hydrophilicity, and higher B-type crystallinity. Addition of clay resulted in hybrid materials with improved properties in relation to TPS alone, even after conditioning at a high relative humidity for 90 days. X-ray diffraction was also used to evaluate clay intercalation within the polymeric matrix, before and after conditioning. Soil burial biodegradation tests, carried out for TPS alone and for TPS/Cloisite 30B hybrids, and followed by weight loss measurements, revealed that biodegradation was enhanced for the hybrid materials in comparison with TPS.

1. Introduction

Polymer/clay hybrid nanocomposites have attracted considerable attention from industries and researchers over the last decade. Silicates like montmorillonite, hectorite, and saponite have been successfully used as reinforcing materials for polymers. This is because of their potential ability to be exfoliated and dispersed within the polymeric matrix. Properly treated, their layer structure can be transformed, at least partially, into platelets with nanometric dimensions and high aspect ratios, which can afford properties enhancements. When compared to conventional composites, improvements have been reported in stiffness and toughness, solvent and UV resistance, gas barrier properties, thermal stability and flame retardancy. Many studies have been carried out on the preparation and characterization of synthetic polymers/clay nanocomposites, and have been reviewed recently (Alexandre & Dubois, 2000; Hussain, Hojjati, Okamoto, & Gorga, 2006; Ray & Okamoto, 2003).

Melt-processing is a recommended route for obtaining well-dispersed exfoliated clay within polymeric matrices. In contrast to in-situ polymerization of intercalated monomers, and intercalation from solution, melt processing can lead to nanocomposites without the addition of solvent (Bousmina, 2006; Cho & Paul, 2001; Homminga, Goderis, Hoffman, Reynaers, & Groeninckx, 2005b).

Nowadays, environmentally friendly processes and products are highly regarded, due to growing concerns about pollution. Natural polymers, such as starch, are biodegradable and renewable raw materials. Starch is a major energy source in the human diet and has been used extensively in the food industry. However, there is an increasing interest in nonfood uses of starch, for example to substitute synthetic polymers. This is because of its total biodegradability and worldwide availability at low cost.

Native starch can be transformed into a thermoplastic material (TPS) through thermomechanical treatment in the presence of suitable plasticizers, such as water and glycerol. The sensitivity of TPS to the humidity atmosphere has been a drawback for its commercial use because its mechanical behavior is dependent on water content (van Soest, Benes, de Wit, & Vliegenthart, 1996a).

Recently, melt processing of starch and clays has been investigated (Chen & Evans, 2005; Chiou et al., 2006; Dean, Yu, & Wu, 2007; Huang & Yu, 2006; Huang, Yu, & Ma, 2004, 2006; Huang, Yu, Ma, & Jin, 2005; Park, Lee, Park, Cho, & Ha, 2003; Zhang, Yu, Xie, Naito, & Kagawa, 2007). X-ray diffraction, scanning and transmission electron microscopy were used to investigate dispersion and exfoliation of clays within starch matrices from various sources. The effect of processing conditions (Chiou et al., 2006) and of the type and content of clay (Huang & Yu, 2006; Park et al., 2003) on properties of nanocomposites were evaluated. High levels of plasticizers and two-step extrusion procedures were used by some of those authors. However, the effect of clay on aging and biodegradation properties has not been addressed.

In this work, regular corn starch plasticized with glycerol was extruded with addition of different amounts of two types of clay. The effects of clay content and of glycerol content on the hydrophilicity of the materials were investigated. Aging of extruded TPS and

---

* Corresponding author. Tel.: +55 21 2562 7208; fax: +55 21 2270 1317.
E-mail address: ctandrade@ima.ufrj.br (C.T. Andrade).

0144-8617/$ - see front matter © 2008 Elsevier Ltd. All rights reserved.
doi:10.1016/j.carbpol.2008.09.020

hybrid materials was accompanied after conditioning at 28 °C and 80% relative humidity for three months by X-ray diffraction measurements. Biodegradation of materials were evaluated by soil burial tests, and their morphology visualized by scanning electron microscopy.

2. Experimental section

2.1. Materials

Regular corn starch (CS) composed of 26–30% amylose and 74–70% amylopectin, and with less than 0.5% gluten, and 12% moisture content was supplied by Corn Products Brazil (São Paulo, SP, Brazil). Analytical grade glycerol was purchased from Vetec Química Fina Ltda. (Rio de Janeiro, RJ, Brazil) and was used as received. Naturally occurring sodium montmorillonite (Na^+MMT, Volclay®) was supplied by Bentonita União do Nordeste S.A. (Campina Grande, PB, Brazil). The cation exchange capacity (CEC) of Na^+MMT was 95 meq/100 g. Organophylic clay Cloisite® 30B (Cloisite 30B), modified with methyl tallow bis-2-hydroxyethyl quaternary ammonium cations, and with a CEC of 100 meq/100 g, was from Southern Clay Product Inc. (Gonzales, TX, USA).

2.2. Preparation of samples

CS and glycerol were premixed in a conventional mixer (Ika Works, Wilmington, NC, USA) for 10 min, and maintained in tightly sealed bags for 10 days at 4 °C. Clay was mixed with CS/glycerol premixtures shortly before extrusion.

2.3. Processing

Plasticized CS and CS/clay mixtures were manually fed and processed in a Haake Rheocord 9000 system (Karlsruhe, Germany), equipped with a single-screw extruder, and four heating zones. The barrel length-to-diameter ratio was 25:1. The screw speed was maintained constant at 40 rpm, and the temperatures of the heating zones were 90, 105, 105, and 90 °C from feed zone to die end. The samples were extruded into a sheet through a 25.0 × 1.0 mm die.

2.4. Contact angle measurements

The effect of clay addition to TPS was investigated by water contact angle measurements with a NRL A-100-00 Ramé-Hart Goniometer (Mountain Lakes, USA). A 2.5 μl droplet of water was applied on the surface of TPS and TPS/clay hybrids. The evolution of the droplet shape was recorded every second by a video camera; and image analysis software was used to determine the contact angle.

2.5. X-ray diffraction (XRD)

XRD curves for Na^+MMT, Cloisite 30B, native CS, TPS, and TPS/clay hybrids were obtained with a Miniflex diffractometer (Rigaku Corporation, Osaka, Japan) operating at CuKα wavelength of 1.542 Å. The samples were exposed to the X-ray beam with the X-ray generator running at 30 kV and 15 mA. Scattered radiation was detected at ambient temperature in the angular region (2θ) of 1–35° at a rate of 1°/min and a step size of 0.05°. Diffractograms were smoothed (Savitsky–Golay, polynome = 2, points = 7), and the baseline was corrected. The relative crystallinity of types B and V_H were determined according to the method described in the literature (Hulleman, Kalisvaart, Janssen, Feil, & Vliegenthart, 1999), by dividing the height of the crystalline peak, around 17° (2θ) and 19° (2θ), respectively, by the total height from the baseline. XRD curves for TPS and TPS/clay hybrids were obtained before and after conditioning at 28 °C and 80% RH, in a climate-controlled chamber M.S. Mistura, model MS 012 (Rio de Janeiro, RJ, Brazil), for 90 days.

2.6. Soil burial biodegradation test

Biodegradation of TPS and TPS/Cloisite 30B hybrids were studied by soil burial test under laboratory conditions (average temperature of 23 °C). Black subsoil was enriched with 30 wt% bovine manure. The initial pH of the soil was 7.3, and the final pH was 6.5. Samples were cut into pieces with 25 × 25 × 1.0 mm dimensions, weighed (0.70 ± 0.05 g), and buried in plastic containers (10 L) filled with soil, previously passed through a 2 mm sieve. Every 15 or 30 days, for a period of 210 days, five replications of each sample were taken out of the container, cleaned with a smooth brush, and weighed. The average weight was considered. Periodically, the soil moisture content was measured; an average value of 16 wt% was maintained during the period of the test. Weight loss of the specimens with time was used to evaluate degradation.

2.7. Scanning electron microscopy

The morphology of the samples was observed with a Jeol electron microscopy, model JSM-5610LV (Akishima-shi, Japan) at

Table 1
Coded levels for the central composite design

Independent variables	Levels				
	$-\alpha$[a]	-1	0	+1	$+\alpha$[a]
Clay content[b] (wt%)	0.34	2.0	6.0	10.0	11.65
Glycerol content[b] (wt%)	20.75	22.0	25.0	28.0	29.24

[a] α = 1.414.
[b] Clay content and glycerol content were based on corn starch dry fraction.

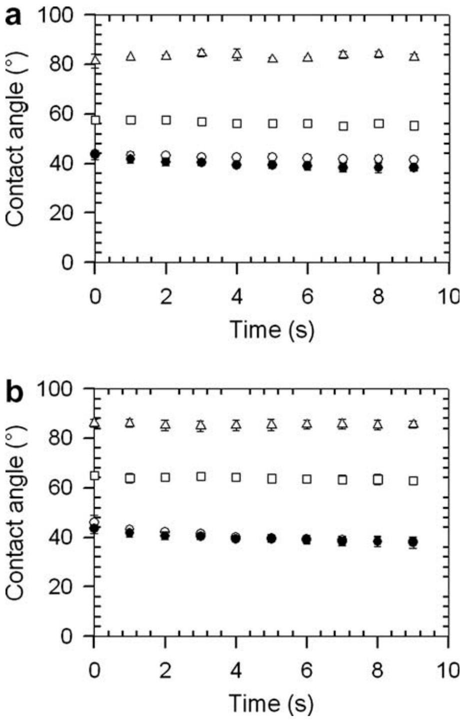

Fig. 1. Evolution of contact angles as a function of time for TPS alone (●), and for TPS/Na^+MMT (a) and TPS/Cloisite 30B (b) hybrid materials, plasticized with 25 wt% glycerol; (○) 0.34 wt% clay, (□) 6.0 wt% clay, (Δ) 11.65 wt% clay.

acceleration voltages of 5 or 15 kV. Samples were cooled in liquid nitrogen, and then fractured. The fractured surfaces were vacuum-coated with gold before measurements.

2.8. Experimental design and statistical analysis

A central composite design was constructed on five levels of two independent variables, i.e. clay content and glycerol content. The design comprised twelve combinations of variable levels for each type of clay, with four replications at the central point (Table 1). The parameters ranges were chosen on the basis of preliminary experiments, performed in an internal mixer.

The response variables were average contact angle, and B-type crystallinity determined before conditioning and after conditioning for 30, 60, and 90 days, at 28 °C and 80% RH, as described previously. A second-order polynomial model for dependent variables was established to fit the experimental data. The analysis of variance (ANOVA) was carried out using Statistica for Windows 6.0 (Statsoft Inc., Tulsa, OK, USA) to determine the significance at the 5% ($P \leqslant 0.05$) level, for linear, quadratic and interaction effects.

3. Results and discussion

All films prepared by melt-extrusion were homogeneous and transparent, which suggests low degree of crystallinity, and well-dispersed particles within the starch matrix.

The wettability properties of a material can be evaluated by the measurement of contact angle of a water drop deposited on the surface of the solid (Roman-Gutierrez, Sabathier, Guilbert, Galet, & Cuq, 2003). Contact angle measurements were carried out for TPS and TPS/clay samples. For both clays, the ANOVA revealed significant effects of clay content and glycerol content on average contact angle. The positive linear effect of clay content and the negative linear effect of glycerol content were the most significant ($P < 0.001$). As expected, the increase in glycerol content led to decreasing average contact angles. Fig. 1(a) and (b) show the evolution of contact angle as a function of time for TPS/Na^+MMT and for TPS/Cloisite 30B materials, plasticized with 25 wt% glycerol, respectively. In each figure, the result for TPS alone was included for comparison. In both cases, increasing contact angles were determined for the samples as the clay content was increased. According to the results, addition of both clays led to materials with lower hydrophilicities than TPS alone. Cloisite 30B was the most effective, and average contact angle reached the highest value (81°) for the composite with 11.65 wt% of this organically-modified clay.

The results from contact angle measurements corroborate published data on water absorption of TPS nanocomposites. Water absorption was evaluated for glycerol-plasticized corn starch/Na^+MMT materials after conditioning at 50% RH. For the highest content of clay (30 wt%), a longer period of time was necessary

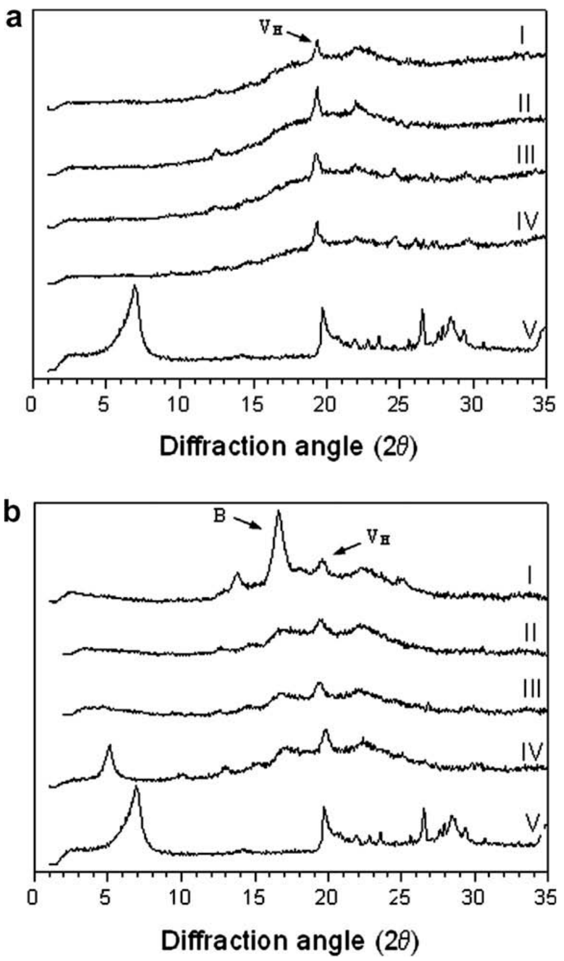

Fig. 2. X-ray diffractograms for TPS alone (trace I), for neat Na^+MMT (trace V), and for TPS/Na^+MMT hybrids with 0.34 wt% clay (trace II), with 6.0 wt% clay (trace III), and with 11.6 wt% clay (trace IV), before conditioning (a), and after conditioning for 90 days (b). TPS and hybrid materials were plasticized with 25 wt% glycerol.

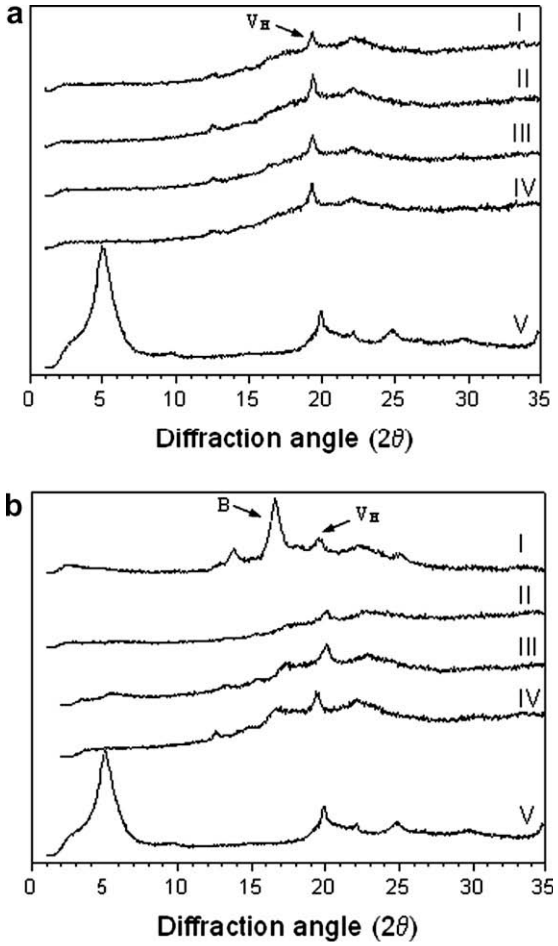

Fig. 3. X-ray diffractograms for TPS alone (trace I), for neat Cloisite 30B (trace V), and for TPS/Cloisite 30B hybrids with 0.34 wt% clay (trace II), with 6.0 wt% clay (trace III), and with 11.6 wt% clay (trace IV), before conditioning (a) and after conditioning for 90 days (b). TPS and hybrid materials were plasticized with 25 wt% glycerol.

to reach equilibrium, and the lowest total content of water was absorbed (Huang et al., 2004).

The crystallinity of TPS alone and hybrid materials was investigated by XRD, before and after conditioning. These experiments are important because plasticized starch has sufficient mobility to recrystallize (retrograded). Addition of layered silicate might contribute to increase nucleation and growth of crystallites with aging, which was not of interest.

Figs. 2 and 3 show diffractograms for TPS alone and TPS/clay hybrids, before and after condition. No residual A-type crystallinity was observed for extruded samples. This result indicates that shear and temperature conditions during extrusion were adequate to melt granular crystallites. The characteristic peak around 19° (2θ), attributed to processing-induced crystallinity of single helical amylose, and denoted as V_H, was observed for all samples. This peak was found in extruded and compression-molded TPS with more than 10% water (van Soest, Hulleman, de Wit, & Vliegenthart, 1996b).

In general, TPS materials present a peak around 17° (2θ), which increases in intensity with aging, attributed to the B-type double helical crystal structures of amylose, and for still longer periods to amylopectin (van Soest et al., 1996b). For TPS alone, although V_H-type relative crystallinity was maintained nearly constant, a B-type relative crystallinity value of 44% was determined after aging for 90 days (Figs. 2b and 3b).

For TPS/Na$^+$MMT and TPS/Cloisite 30B samples, ANOVA revealed a significant effect of glycerol content on B-type relative crystallinity. For both types of materials, glycerol content exerted a positive linear effect on B-type crystallinity.

No B-type crystallinity peak around 17° (2θ) was detected for samples that had not been submitted to 80% relative humidity condition, and had been measured after 5 days of processing (Figs. 2a and 3a). Although the peak attributed to B-type crystallinity increased significantly in intensity for TPS alone after 90 days of conditioning, only a slight increase in B-type crystallinity was observed for the hybrids (Figs. 2b and 3b, traces II–IV).

For some polymer/nanoclay systems, nucleation of matrix crystallization was observed at low levels of clay addition (Homminga, Goderis, Dolbnya, & Groeninckx, 2006; Homminga, Goderis, Dolbnya, Reynaers, & Groeninckx, 2005a; Lincoln, Vaia, & Krishna-

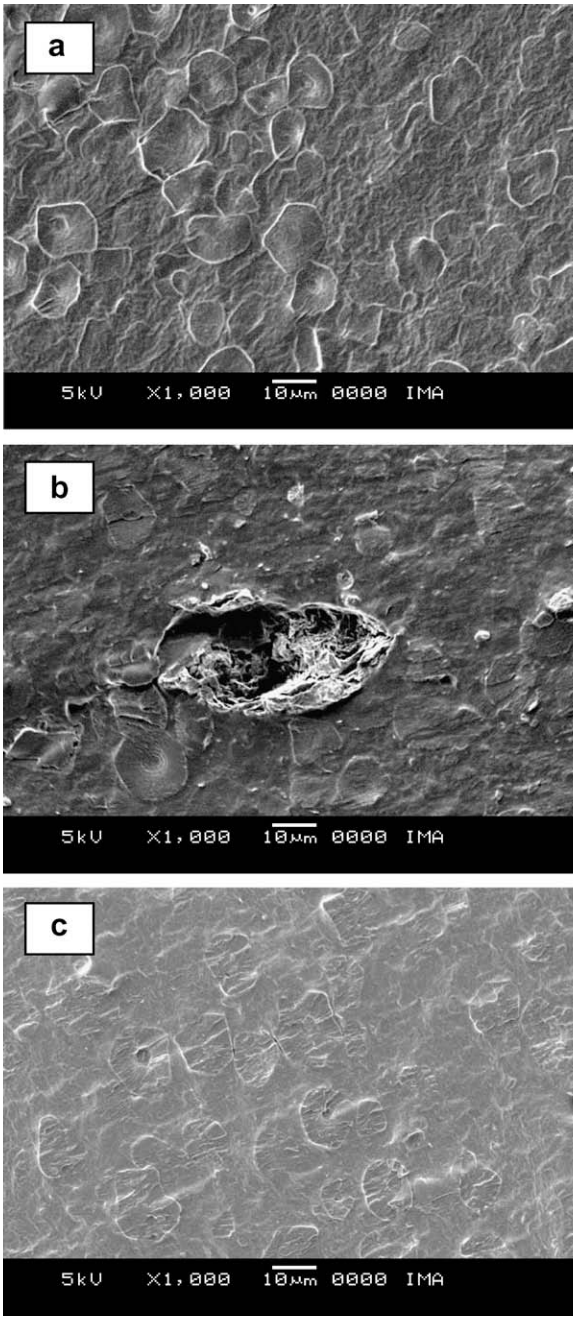

Fig. 4. SEM images for fractured surfaces of TPS alone (a), TPS/6.0 wt% Na$^+$MMT (b), and TPS/6.0 wt% Cloisite 30B (c) hybrids, plasticized with 25 wt% glycerol.

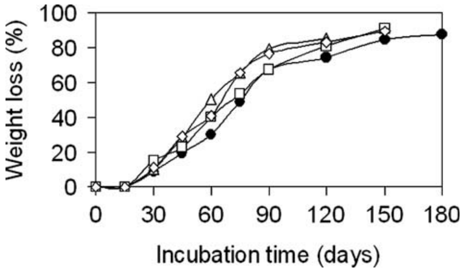

Fig. 5. Weight loss for TPS alone (●), and for TPS/Cloisite 30B hybrids, plasticized with 25 wt% glycerol, with 0.34 wt% clay (Δ), with 6.0 wt% clay (□), and with 11.65 wt% clay (◇).

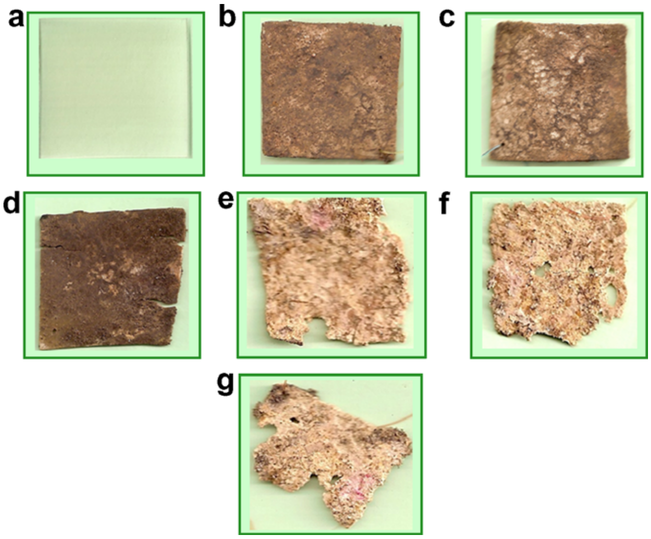

Fig. 6. Photographs for TPS/Cloisite 30B hybrids, plasticized with 25 wt% glycerol; before soil burial (a); after soil burial for 15 days (b), for 30 days (c), for 45 days (d), for 60 days (e), for 90 days (f), and for 120 days (g).

moorti, 2004;). However, at a sufficiently high level of nanoparticle addition, silicate platelets disturb crystal growth, and retardation of the crystalline rate was observed (Fornes & Paul, 2003; Homminga et al., 2005a, 2006). In this study, reduced relative crystallinities were observed for the TPS/clay hybrids, in relation to TPS alone, independently of clay type. Well-dispersed particles within the polymeric matrix may have retarded and unfavored regular packing of starch macromolecules helices. The difference in crys-

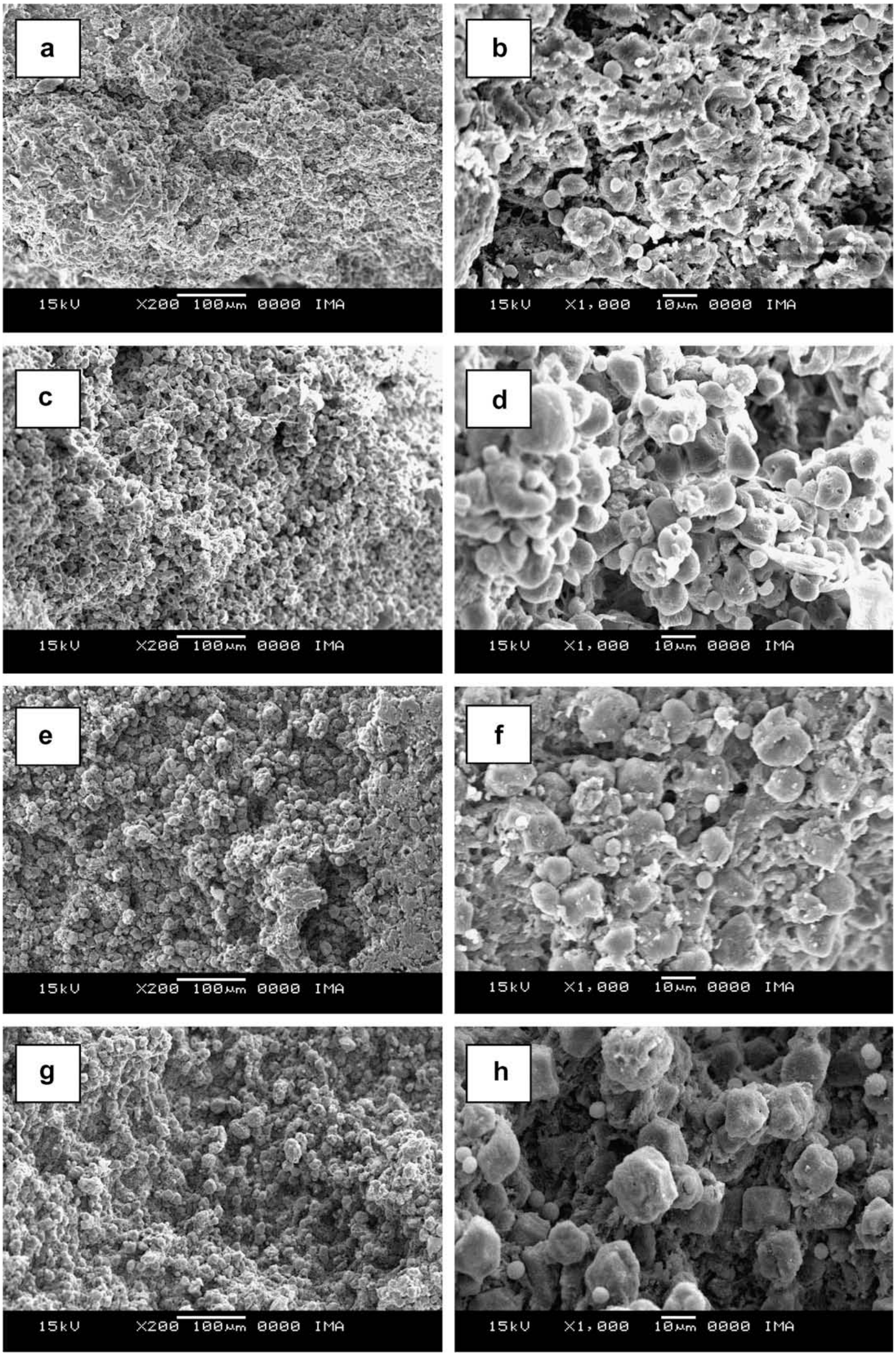

Fig. 7. SEM images for fractured surfaces of materials after incubation for 120 days; TPS alone (a and b), and for TPS/Cloisite 30B hybrids with 0.34 wt% clay (c and d), with 6.0 wt% clay (e and f), and with 11.65 wt% clay (g and h). TPS and hybrid materials were plasticized with 25 wt% glycerol.

tallization behavior between synthetic polymers and TPS may be attributed to the higher molecular weight of starch macromolecules.

Figs. 2 and 3 also allow the comparison of XRD patterns for Na^+MMT and Cloisite 30B, with the respective diffractograms obtained for the hybrid materials. The XRD curve for Na^+MMT (Fig. 2, trace V) shows a peak at 7.0° (2θ), corresponding to an interlayer basal spacing (d_{001}-spacing) of 1.3 nm. For TPS/Na^+MMT hybrids measured before conditioning, no diffraction peak within the 1–10° (2θ) range was observed. Although no crystalline peak was observed for conditioned hybrids with 0.34 wt% Na^+MMT, intercalated structures was evidenced by XRD peaks for other conditioned samples with higher concentrations of clay.

In Fig. 3, for neat Cloisite 30B (trace V), a high-intensity crystalline peak was detected at 5.0° (2θ), which corresponds to a d_{001}-spacing of 1.8 nm. No diffraction peak within that 2θ range was observed for TPS/Cloisite 30B nanocomposites. The absence of the characteristic diffraction peak suggests a highly exfoliated structure with dispersed silicate layers, independently of clay content, and of aging. Considering that a strong starch polymers/surfactant affinity was not expected, the higher exfoliation degree observed for these hybrids may be attributed to the larger platelets spacing of the organically-modified clay.

Scanning electron microscopy (SEM) was used to investigate the morphology of TPS and TPS/clay hybrids. Fig. 4a shows the micrograph of the fractured surface of a TPS sample, processed with 25 wt% glycerol. In this figure, surface features consist of ghosts (the remaining part of the starch granule), embebbed in a matrix composed mostly of amylose (Fannon & BeMiller, 1992; Prentice, Stark, & Gidley, 1992; Thiré, Simão, & Andrade, 2003). At the same magnification, Fig. 4(b and c) show the morphology of fractured surfaces of TPS/Na^+MMT and TPS/Cloisite 30B hybrids, respectively, with 6.0 wt% clay. Although XRD had suggested the exfoliation of silicate layers within the TPS matrix, for these samples, at least for the TPS/Na^+MMT sample with 6 wt% clay, a 50 μm tactoid may be observed in Fig. 4b. No such feature was observed for TPS filled with Cloisite 30B at 6 wt% concentration, which corroborates the XRD data on the higher level of exfoliated silicate layers for this hybrid with the organically-modified clay.

Biodegradation experiments are of fundamental importance for the production of environmentally friendly materials (Chiellini, Corti, D'Antone, & Billingham, 2007). The effect of clay addition on biodegradation behavior of the nanocomposites was investigated. Starch is a well-known biodegradable material. Submitted to soil burial test, a thin film of corn starch presented complete degradation after 60 days (Guohua et al., 2006). In this work, TPS/Cloisite 30B nanocomposites, prepared in a single-screw extruder with 25 wt% glycerol, were chosen for the biodegradation studies. Tests were carried out at room temperature, and evaluated by weighing specimens, after being buried in composted soil. The variation in weight loss is shown in Fig. 5. For TPS alone and for TPS/Cloisite 30B nanocomposites, curves of the same type were found, with no weight loss along the first 15 days of incubation. A time lag before the beginning of biodegradation in soil was also observed for another biopolymer, and was attributed to the adaptation of the microorganism population to the new polymeric environment (Iovino, Zullo, Rao, Cassar, & Gianfreda, 2008).

The biodegradation rate of TPS was enhanced significantly by addition of Cloisite 30B. TPS samples could be weighed up to 180 days (~87% degradation), whereas nanocomposite samples with 0.34 wt% clay could only be weighed up to 120 days (85 wt% degradation) because of specimens fragility. In a study reported recently for poly(hydroxy butyrate) and its nanocomposites with organically-modified synthetic fluoromica, submitted to soil burial tests, the rate and degree of biodegradation were also favored in the presence of clay (Maiti, Batt, & Giannelis, 2007). In this work, the effect of starch matrix retrogradation seems to influence the biodegradation rate. From the 60th day of incubation, the nanocomposite that exhibited the most rapid weight loss was that with 0.34 wt% clay. The fastest biodegradation of this material was probably due to its lower relative crystallinity, and higher hydrophilicity.

Fig. 6 shows photographs taken for TPS/034 wt% Cloisite 30B samples, as a function of incubation time. The specimens showed a gradual change in color, thickness, surface roughness, and increasing erosion, as mineralization progressed.

SEM was also used to image samples at an advanced stage of biodegradation in soil. Fig. 7(a–h) show SEM images for fractured surfaces of TPS alone, and for TPS/Cloisite 30B nanocomposites. Low magnification micrographs revealed cracks, formed as a result of mineralization of the polymeric matrix (Ikada, 1999). At a higher magnification, a heterogeneous bacterial community, characteristics of biodegradation in compost soil, may be observed.

4. Conclusion

TPS and TPS/clay hybrids, plasticized with glycerol, were prepared by melt-extrusion in a single-screw extruder under the same conditions. Natural Na^+MMT and organophylic Cloisite® 30B were used. A central composite design was constructed to investigate the effect of clay content and of glycerol content on the hydrophilicity, and B-type crystallinity of nanocomposites. Contact angle measurements and XRD results revealed that the increase in glycerol content led to materials with higher hydrophilicity and B-type crystallinity. Contrarily, addition of clay may be a way of solving, at least in part, the main drawbacks to the use of starch-based bioplastics. Both clays contributed to lower hydrophilicity and to retard starch matrix retrogradation. For materials plasticized with 25 wt% glycerol, XRD results revealed the appearance of the characteristic diffraction peak of intercalated Na^+MMT with aging. The absence of the characteristic XRD peak, and the homogeneous matrix observed by SEM, suggested that the hybrids based on Cloisite® 30B displayed a high degree of exfoliation. Results from soil burial tests showed that the addition of the organically-modified clay contributed to increase the biodegradation rate of nanocomposites, in comparison with TPS alone. Biodegradation in soil was dependent on the relative crystallinity of the polymeric matrix, and on the sample hydrophilicity.

Acknowledgements

The authors thank the financial support of Conselho Nacional para o Desenvolvimento Científico e Tecnológico (CNPq), Fundação de Amparo à Pesquisa do Estado do Rio de Janeiro (Processo no E-26/152.719/2006), and Projeto Encomenda Transversal FINEP/01.06.1208.00 – Ref. 3733/06.

References

Alexandre, M., & Dubois, P. (2000). Polymer-layered silicate nanocomposites: Preparation, properties and uses of a new class of materials. *Materials Science and Engineering, 28*, 1–63.

Bousmina, M. (2006). Study of intercalation and exfoliation processes in polymer. *Macromolecules, 39*, 4259–4263.

Chen, B., & Evans, J. R. G. (2005). Thermoplastic starch-clay nanocomposites and their characteristics. *Carbohydrate Polymers, 61*, 455–463.

Chiellini, E., Corti, A., D'Antone, S., & Billingham, N. C. (2007). Microbial biomass yield and turnover in soil biodegradation tests: Carbon substrate effects. *Journal of Polymers and the Environment, 15*, 169–178.

Chiou, B.-S., Yee, E., Wood, D., Shey, J., Glenn, G., & Orts, W. (2006). Effects of processing conditions on nanoclay dispersion in starch-clay nanocomposites. *Cereal Chemistry, 83*, 300–305.

Cho, J. W., & Paul, D. R. (2001). Nylon 6 nanocomposites by melt compounding. *Polymer, 42*, 1083–1094.

Dean, K., Yu, L., & Wu, D. Y. (2007). Preparation and characterization of melt-extruded thermoplastic starch/clay nanocomposites. *Composites Science and Technology, 67*, 413–421.

Fannon, J. E., & BeMiller, J. N. (1992). Structure of corn starch paste and granule remnants revealed by low-temperature scanning electron microscopy after cryopreparation. *Cereal Chemistry, 69*, 456–460.

Fornes, T. D., & Paul, D. R. (2003). Crystallization behavior of nylon 6 nanocomposites. *Polymer, 44*, 3945–3961.

Guohua, Z., Ya, L., Cuilan, F., Min, Z., Caiqiong, Z., & Zongdao, C. (2006). Water resistance, mechanical properties and biodegradability of methylated-cornstarch/poly(vinyl alcohol) blend film. *Polymer Degradation and Stability, 91*, 703–711.

Homminga, D., Goderis, B., Dolbnya, I., & Groeninckx, G. (2006). Crystallization behavior of polymer/montmorillonite nanocomposites. Part II. Intercalated poly(ε-caprolactone)/montmorillonite nanocomposites. *Polymer, 47*, 1620–1629.

Homminga, D., Goderis, B., Dolbnya, I., Reynaers, H., & Groeninckx, G. (2005a). Crystallization behavior of polymer/montmorillonite nanocomposites. Part I. Intercalated poly(ethylene oxide)/montmorillonite nanocomposites. *Polymer, 46*, 11359–11365.

Homminga, D., Goderis, B., Hoffman, S., Reynaers, H., & Groeninckx, G. (2005b). Influence of shear flow on the preparation of polymer layered silicate nanocomposites. *Polymer, 46*, 9941–9954.

Huang, M., & Yu, J. (2006). Structure and properties of thermoplastic corn starch/montmorillonite biodegradable composites. *Journal of Applied Polymer Science, 99*, 170–176.

Huang, M., Yu, J., & Ma, X. (2004). Studies on properties of montmorillonite-reinforced thermoplastic starch composites. *Polymer, 45*, 7017–7023.

Huang, M., Yu, J., & Ma, X. (2006). High mechanical performance MMT-urea and formamide-plasticized thermoplastic cornstarch biodegradable nanocomposites. *Carbohydrate Polymers, 63*, 393–399.

Huang, M., Yu, J., Ma, X., & Jin, P. (2005). High performance biodegradable thermoplastic starch-EMMT nanoplastics. *Polymer, 46*, 3157–3162.

Hulleman, S. H. D., Kalisvaart, M. G., Janssen, F. H. P., Feil, H., & Vliengenthart, J. F. G. (1999). Origins of B-type crystallinity in glycerol-plasticised, compression-moulded potato starches. *Carbohydrate Polymers, 39*, 351–360.

Hussain, F., Hojjati, M., Okamoto, M., & Gorga, R. E. (2006). Polymer-matrix nanocomposites, processing, manufacturing and application: An overview. *Journal of Composite Materials, 40*, 1511–1575.

Ikada, E. (1999). Electron microscope observation of biodegradation of polymers. *Journal of Environmental Polymer Degradation, 7*, 197–201.

Iovino, R., Zullo, R., Rao, M. A., Cassar, L., & Gianfreda, L. (2008). Biodegradation of poly(lactic acid)/starch/coir biocomposites under controlled composting conditions. *Polymer Degradation and Stability, 93*, 147–157.

Lincoln, D. M., Vaia, R. A., & Krishnamoorti, R. (2004). Isothermal crystallization of nylon-6/montmorillonite nanocomposites. *Macromolecules, 37*, 4554–4561.

Maiti, P., Batt, C. A., & Giannelis, E. P. (2007). New biodegradable polyhydroxybutyrate/layered silicate nanocomposites. *Biomacromolecules, 8*, 3393–3400.

Park, H.-M., Lee, W., Park, C.-Y., Cho, W.-J., & Ha, C.-S. (2003). Environmentally friendly hybrids. Part I. Mechanical, thermal, and barrier properties of thermoplastic starch/clay nanocomposites. *Journal of Materials Science, 38*, 909–915.

Prentice, R. D. M., Stark, J. R., & Gidley, M. J. (1992). Granule residues and ghosts remaining after heating A-type barley-starch granules in water. *Carbohydrate Research, 227*, 121–130.

Ray, S. S., & Okamoto, M. (2003). Polymer/layered nanocomposites: A review from preparation to processing. *Progress in Polymer Science, 28*, 1539–1641.

Roman-Gutierrez, A., Sabathier, J., Guilbert, S., Galet, L., & Cuq, B. (2003). Characterization of the surface hydration properties of wheat flours and flour components by the measurement of contact angle. *Powder Technology, 129*, 37–45.

Thiré, R. M. S. M., Simão, R. A., & Andrade, C. T. (2003). High resolution imaging of the microstructure of maize starch films. *Carbohydrate Polymers, 54*, 149–158.

van Soest, J. J. G., Benes, K., de Wit, D., & Vliegenthart, J. F. G. (1996a). The influence of starch molecular mass on the properties of extruded thermoplastic starch. *Polymer, 37*, 3543–3552.

van Soest, J. J. G., Hulleman, S. H. D., de Wit, D., & Vliegenthart, J. F. G. (1996b). Crystallinity in starch plastics. *Industrial Crops and Products, 5*, 11–22.

Zhang, Q.-X., Yu, Z.-Z., Xie, X.-L., Naito, K., & Kagawa, Y. (2007). Preparation and crystalline morphology of biodegradable starch/clay nanocomposites. *Polymer, 48*, 7193–7200.